450 cm^{-1} (ν_2).) This points to a lowering of the T_d symmetry of the SO_4^{2-} ion, possibly due to bidentate coordination, as judged from the number of bands in the range 1000–1300 cm^{-1}.[22] The IR spectrum of $Cs_2S_2O_7$ (spectrum A in Figure 4) exhibits the same features as that of $K_2S_2O_7$, and the frequencies listed in Table II agree very well with the frequencies observed previously[12] for $K_2S_2O_7$. By comparison with spectrum B in Figure 4, strong bands due to $S_2O_7^{2-}$ in the proposed compound, $Cs_4(VO_2)_2(SO_4)_2S_2O_7$, might be located at the highest frequencies, i.e. 1250–1300 cm^{-1}, and around 775 and 575 cm^{-1}. The strong and narrow band found for $Cs_2S_2O_7$ at 1040 cm^{-1} might be the strong band found at 1024 cm^{-1} in spectrum B. It is characteristic that all of the strong bands found for the $S_2O_7^{2-}$ ion in $Cs_2S_2O_7$ are shifted somewhat in frequency and split into more components, probably due to the coordination to the central vanadium atom in the complex compound. The two IR-active stretching modes for the bent VO_2^+ entity are found in the range 1030–875 cm^{-1}, depending on the type of ligands connected to the metal.[23-25] The bending mode of VO_2^+ is found in the range 300–400 cm^{-1}, which is out of the range measured here. The stretching bands for the vanadium–ligand bonds are typically found in the range 400–600 cm^{-1}.[23-25] Due to the very large number of bands found for the $Cs_4(VO_2)_2(SO_4)_2S_2O_7$ compound and the overlapping regions of the free-group vibrations of the complex components, it is—as shown in Table II—not possible to make a definite assignment of the bands to specific groups. However, the IR spectra are in agreement with the proposed formula, $Cs_4(VO_2)_2(SO_4)_2S_2O_7$, for the compound.

Further considerations of the conductivity and complex formation in the molten $Cs_2S_2O_7$–V_2O_5 system will be published[26] when the molar conductivities can be calculated from ongoing density measurements of the molten $Cs_2S_2O_7$–V_2O_5 system.

Acknowledgment. Chresten Traeholt, Laboratory of Applied Physics, The Technical University of Denmark, is gratefully acknowledged for conducting the EDS experiments. Further thanks are due to The Danish Technical Research Council, The Danish Natural Science Research Council, and the Henriksens Foundation, which have supported this investigation.

Registry No. $Cs_2S_2O_7$, 50992-48-8; V_2O_5, 1314-62-1; $Cs_4(VO_2)_2(SO_4)_2S_2O_7$, 84662-69-1.

Supplementary Material Available: Table A, listing all measured specific conductivities and temperatures for each of the investigated compositions of the $Cs_2S_2O_7$–V_2O_5 system, Figure A, outlining the experimental evidence of partial crystallization, and Figure B, showing the thermograms obtained on the $Cs_2S_2O_7$–V_2O_5 system (8 pages). Ordering information is given on any current masthead page.

(23) Weidlein, J.; Dehnicke, K. *Z. Anorg. Allg. Chem.* **1966**, *348*, 278.
(24) Griffith, W. P.; Wicking, T. D. *J. Chem. Soc. A* **1968**, 400.
(25) Pausewang, G.; Dehnicke, K. *Z. Anorg. Allg. Chem.* **1968**, *369*, 265.
(26) Folkmann, G. E.; Hatem, G.; Fehrmann, R.; Gaune-Escard, M.; Bjerrum, N. J. Submitted for publication.

Contribution from Lehrstuhl für Anorganische Chemie I,
Ruhr-Universität, D-4630 Bochum, FRG

Switching the Mechanism of Spin-Exchange Coupling in (μ-Oxo)bis(μ-carboxylato)divanadium(III) Complexes by Protonation of the Oxo Bridge

Petra Knopp and Karl Wieghardt*

Received February 5, 1991

Hydrolysis of $LVCl_3$ in methanol/water (4:1) mixtures with the sodium salts of a variety of carboxylic acids (CF_3COOH, FCH_2CO_2H, $ClCH_2CO_2H$, $BrCH_2CO_2H$, HCO_2H, CH_3COOH, C_6H_5COOH) affords green dinuclear complexes $[L_2V^{III}_2(\mu\text{-O})(\mu\text{-carboxylato})_2]^{2+}$, which have been isolated as solid hexafluorophosphate or iodide salts (L = 1,4,7-trimethyl-1,4,7-triazacyclononane, $C_9H_{21}N_3$). From temperature-dependent magnetic susceptibility measurements it was found that the spins of both vanadium(III) ions (d^2) are fully aligned between 10 and 298 K, indicating very strong intramolecular ferromagnetic coupling. From CH_3CN solutions of these green complexes the pink protonated forms $[L_2V^{III}_2(\mu\text{-OH})(\mu\text{-carboxylato})_2]^{3+}$ are generated by addition of concentrated HBr or $HClO_4$. $[L_2V_2(\mu\text{-OH})(\mu\text{-}C_6H_5CO_2)_2]Br_3$ and $[L_2V_2(\mu\text{-OH})(\mu\text{-}CH_3CO_2)_2](ClO_4)_3\cdot H_2O$ have been isolated as red crystals. The former exhibits intramolecular antiferromagnetic spin-exchange coupling ($H = -2JS_1\cdot S_2$, $S_1 = S_2 = 1$; $J = -36$ cm^{-1}, $g = 1.87$). A model is presented to rationalize the dramatic change of mechanism of the spin-exchange coupling upon protonation of the μ-oxo group.

Introduction

In recent years we and others have studied a series of homodinuclear complexes containing the (μ-oxo)bis(μ-carboxylato)dimetal(III) core where the metal(III) ions are either first-row transition metals (Ti,[1] V,[2] Cr,[3] Mn,[4] Fe[5]) with the d-electron configuration increasing stepwise from d^1 to d^5 or second-row transition metals (Mo,[6] Ru[7]). As nonbridging ligands, hydro-

(1) Bodner, A.; Drücke, S.; Wieghardt, K.; Nuber, B.; Weiss, J. *Angew. Chem., Int. Ed. Engl.* **1990**, *29*, 68.
(2) (a) Wieghardt, K.; Köppen, M.; Nuber, B.; Weiss, J. *J. Chem. Soc., Chem. Commun.* **1986**, 1530. (b) Köppen, M.; Fresen, G.; Wieghardt, K.; Llusar, R. M.; Nuber, B.; Weiss, J. *Inorg. Chem.* **1988**, *27*, 721. (c) Knopp, P.; Wieghardt, K.; Nuber, B.; Weiss, J.; Sheldrick, W. S. *Inorg. Chem.* **1990**, *29*, 363.
(3) Martin, L. L.; Wieghardt, K.; Blondin, G.; Girerd, J. J.; Nuber, B.; Weiss, J. *J. Chem. Soc., Chem. Commun.* **1990**, 1767.
(4) (a) Wieghardt, K.; Bossek, U.; Ventur, D.; Weiss, J. *J. Chem. Soc., Chem. Commun.* **1985**, 347. (b) Bossek, U.; Wieghardt, K.; Nuber, B.; Weiss, J. *Inorg. Chim. Acta* **1989**, *165*, 123. (c) Sheats, J. E.; Czernuszewicz, R. S.; Dismukes, G. C.; Rheingold, A. L.; Petrouleas, V.; Stubbe, J.; Armstrong, W. H.; Beer, R. H.; Lippard, S. J. *J. Am. Chem. Soc.* **1987**, *109*, 1435. (d) Wieghardt, K.; Bossek, U.; Nuber, B.; Weiss, J.; Bonvoisin, J.; Corbella, M.; Vitols, S. E.; Girerd, J. J. *J. Am. Chem. Soc.* **1988**, *110*, 7398. (e) Wieghardt, K. *Angew. Chem., Int. Ed. Engl.* **1989**, *28*, 1153 and references therein. (f) Ménage, S.; Girerd, J. J.; Gleizes, A. *J. Chem. Soc., Chem. Commun.* **1988**, 431. (g) Vincent, J. B.; Folting, K.; Huffman, J. C.; Christou, G. *Biochem. Soc. Trans.* **1988**, *16*, 822.

0020-1669/91/1330-4061$02.50/0

tris(pyrazolyl)borate and tridentate amines such as 1,4,7-trimethyl-1,4,7-triazacyclononane have been employed to complete the octahedral environment at each metal center. These compounds are ideally suited to study the mechanism of spin-exchange coupling because the different metal ions are held together in identical ligand matrices.

In some instances, it is possible to reversibly protonate the μ-oxo bridge, forming a μ-hydroxo-bridged species (eq 1).[6-10] This

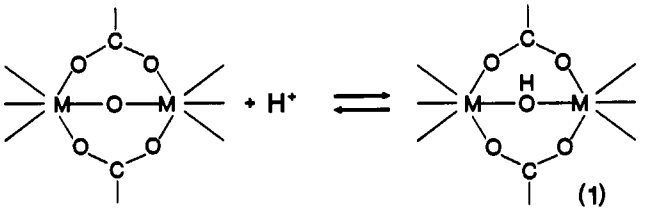

moderate chemical perturbation induces a dramatic change in the degree and, as we will show here, even in the nature of the spin-exchange coupling. Thus in the (μ-oxo)bis(μ-carboxylato)divanadium(III) species[2] it was found that at room temperature the spins of all four unpaired electrons (two at each V(III) center) are fully aligned, indicating a strong intramolecular *ferromagnetic* coupling yielding an $S = 2$ ground state. Protonation at the oxo bridge of these complexes leads to moderately strong intramolecular *antiferromagnetic* coupling ($S = 0$).

Experimental Section

The ligand 1,4,7-trimethyl-1,4,7-triazacyclononane (L) has been synthesized as described previously.[11] All other reagents were purchased from commercial sources and used as received. The syntheses of the complexes $[L_2V_2(\mu\text{-}O)(\mu\text{-}CH_3CO_2)_2]I_2\cdot 2H_2O$ and $[L_2V_2(\mu\text{-}O)(\mu\text{-}C_6H_5CO_2)_2]I_2\cdot 2H_2O$ are also described in the literature.[2]

$LVCl_3$. The preparation of purple $[LVCl_3]$dmf has been described previously.[2a,6] Here we report a synthesis which gives higher yields. A deoxygenated solution of VCl_3 (4.5 g; 28.6 mmol) in dry acetonitrile (30 mL) was heated to reflux for 10 min, after which light green $VCl_3(CH_3CN)_3$ precipitated upon cooling of the solution. To this mixture was added a CH_3CN solution (20 mL) of 1,4,7-trimethyl-1,4,7-triazacyclononane (4.9 g; 28.6 mmol). Heating to reflux for 30 min afforded a purple solution from which purple crystals of $LVCl_3$ precipitated in 95% yield (8.9 g). UV-vis (CH_3CN) λ_{max}, nm (ϵ, L mol^{-1} cm^{-1})): 759 (30), 507 (160), 318 (2.7×10^3).

$[L_2V_2(\mu\text{-}O)(\mu\text{-}O_2CR)_2]^{2+}$ (R = CF_3, CH_2F, CH_2Cl, CH_2Br, H). A general procedure for the synthesis of carboxylato-bridged vanadium(III) complexes is given only. $LVCl_3$ (0.30 g; 0.90 mmol) was dissolved in a methanol/water mixture (4:1) (15 mL) under an argon atmosphere. To this solution was added an excess (1.0 g) of the sodium salt of the respective carboxylic acid. An immediate color change to deep green was observed. After gentle heating to ≈50 °C for 20 min, KPF_6 or NaI (1.0 g) was added, which initiated the precipitation of green microcrystals of the hexafluorophosphate or iodide salt of the desired complex in ≈40% yield.

$[L_2V_2(O)(O_2CCF_3)_2](PF_6)_2\cdot 2H_2O$. Anal. Calcd for $C_{22}H_{46}N_6O_7P_2F_{18}V_2$ (mol wt 1012.45): C, 26.1; H, 4.6; N, 8.3. Found: C, 25.9; H, 4.5; N, 8.2. IR (KBr, cm^{-1}): ν_{as}(C–O) 1653, ν_s(C–O) 1500. UV-vis (CH_3CN) λ_{max}, nm (ϵ, L mol^{-1} cm^{-1}): 679 (2600), 457 (3800), 505 sh, 267 (5100).

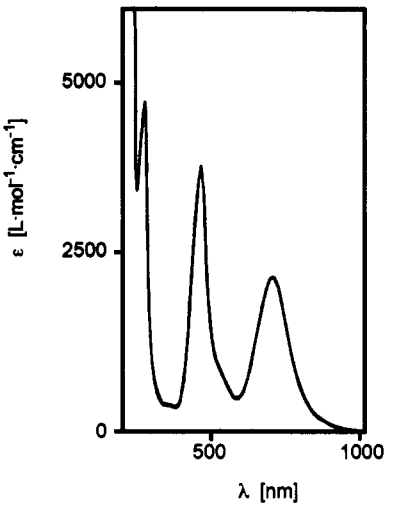

Figure 1. Electronic spectrum of $[L_2V_2(\mu\text{-}O)(\mu\text{-}O_2CCH_2Cl)_2](PF_6)_2$ in CH_3CN at 20 °C.

$[L_2V_2(O)(O_2CCH_2F)_2](PF_6)_2\cdot 2H_2O$. Anal. Calcd for $C_{22}H_{50}N_6O_7P_2F_{14}V_2$ (mol wt 940.48): C, 28.1; H, 5.4; N, 8.9; V, 10.8. Found: C, 27.9; H, 5.3; N, 8.7; V, 11.1. IR (KBr, cm^{-1}): ν_{as}(C–O) 1592, ν_s(C–O) 1467. UV-vis (CH_3CN) λ_{max}, nm (ϵ, L mol^{-1} cm^{-1}): 660 (2100), 452 (3700), 500 sh, 365 (300), 261 (4600). μ_{eff}(293 K) = 4.60 μ_B per dinuclear unit.

$[L_2V_2(O)(O_2CCH_2Cl)_2](PF_6)_2$. Anal. Calcd for $C_{22}H_{46}N_6O_5P_2F_{12}Cl_2V_2$ (mol wt 935.35): C, 28.3; H, 4.7; N, 9.0; V, 10.9; Cl, 7.6. Found: C, 27.9; H, 4.8; N, 8.9; V, 10.7; Cl, 7.4. IR (KBr, cm^{-1}): ν_{as}(C–O) 1592, ν_s(C–O) 1471. UV-vis (CH_3CN) λ_{max}, nm (ϵ, L mol^{-1} cm^{-1}): 698 (2200), 453 (3800), 560 sh, 365 (350), 262 (4700).

$[L_2V_2(O)(O_2CCH_2Br)_2](PF_6)_2$. Anal. Calcd for $C_{22}H_{46}N_6O_5P_2F_{12}Br_2V_2$ (mol wt 1026.26): C, 25.7; H, 4.5; N, 8.2; V, 9.9. Found: C, 25.6; H, 4.4; N, 8.1; V, 10.2 Ir (KBr, cm^{-1}): ν_{as}(C–O) 1590, ν_s(C–O) 1473. UV-vis (CH_3CN) λ_{max}, nm (ϵ, L mol^{-1} cm^{-1}): 698 (2300), 453 (4000), 500 sh, 360 (420), 262 (5000). μ_{eff}(293 K) = 4.68 μ_B per dinuclear unit.

$[L_2V_2(O)(O_2CH)_2]I_2\cdot 2H_2O$. Anal. Calcd for $C_{20}H_{48}N_6O_7I_2V_2$ (mol wt 840.33): C, 28.6; H, 5.8; N, 10.0; V, 12.1. Found: C, 28.5; H, 6.0; N, 9.6; V, 12.3. IR (KBr, cm^{-1}): ν_{as}(C–O) 1571, ν_s(C–O) 1467. UV-vis (CH_3CN) λ_{max}, nm (ϵ, L mol^{-1} cm^{-1}): 698 (2000), 451 (3900), 500 sh, 365 (300).

$[L_2V_2(OH)(O_2CC_6H_5)_2]Br_3$. To a solution of $[L_2V_2(O)(O_2CC_6H_5)_2]I_2\cdot 2H_2O$ (0.5 g; 0.5 mmol) in CH_3CN (10 mL) was added dropwise concentrated HBr (48%) until the color of the solution changed from green to red. Within a few hours at 5 °C, red crystals precipitated, which were collected by filtration and dried in vacuo. Yield: 0.46 g (93%). Anal. Calcd for $C_{32}H_{53}N_6O_5Br_3V_2$ (mol wt 943.41): C, 40.7; H, 5.7; N, 8.9. Found: C, 40.5; H, 5.5; N, 8.8.

$[L_2V_2(OH)(O_2CCH_3)_2](ClO_4)_3\cdot H_2O$. To a solution of $[L_2V_2(O)(O_2CCH_3)_2](ClO_4)_2$ (0.5 g; 0.6 mmol) in CH_3CN (10 mL) was added dropwise concentrated $HClO_4$ until the green color had changed to red. *This procedure is potentially hazardous and was carried out in a hood with appropriate protection!* A brown-red precipitate formed immediately, which was filtered off and dried in vacuo. Yield: 0.48 g (84%). Anal. Calcd for $C_{22}H_{51}N_6O_{18}Cl_3V_2$ (mol wt 895.92): C, 29.5; H, 5.7; N, 9.4. Found: C, 29.4; H, 5.4; N, 9.3.

Physical Measurements. Cyclic voltammograms (CV's) were measured by using the apparatus and procedures described in ref 2. The voltammograms were recorded in CH_3CN solution containing ≈10^{-3} M sample (0.1 M tetra-*n*-butylammonium hexafluorophosphate, [TBA]PF_6, supporting electrolyte, Au-disk working electrode, Ag/AgCl–saturated LiCl in CH_3OH reference electrode). Redox potentials $(E_{p,a} - E_{p,c})/2$ in volts are referenced to the ferrocenium/ferrocene couple as the internal standard. Under our experimental conditions the Fc^+/Fc couple is at $E_{1/2}$ = +0.51 V vs Ag/AgCl. Magnetic susceptibilities of powdered samples were measured by using the Faraday method in the temperature range 90–298 K. Corrections for diamagnetism were applied with use of Pascal's constants. Infrared spectra were recorded in the range 4000–400 cm^{-1} as KBr disks on a Perkin-Elmer FT-IR spectrometer, Model 1720 X. Electronic absorption spectra were recorded on a Perkin-Elmer Lambda 9 spectrophotometer.

Results

Hydrolysis of mononuclear $LVCl_3$ in a methanol/water mixture (4:1) with an excess of the sodium salts of carboxylic acids results in the formation of green dinuclear (μ-oxo)bis(μ-carboxylato)-

(5) Review articles: (a) Lippard, S. J. *Angew. Chem., Int. Ed. Engl.* **1988**, *27*, 344. (b) Kurtz, D. M. *Chem. Rev.* **1990**, *90*, 585. (c) Hartman, J. R.; Rardin, R. L.; Chaudhuri, P.; Pohl, K.; Wieghardt, K.; Nuber, B.; Weiss, J.; Papaefthymiou, G. C.; Frankel, R. B.; Lippard, S. J. *J. Am. Chem. Soc.* **1987**, *109*, 7387.
(6) (a) Neves, A.; Bossek, U.; Wieghardt, K.; Nuber, B.; Weiss, J. *Angew. Chem., Int. Ed. Engl.* **1988**, *27*, 685. (b) Wieghardt, K.; Bossek, U.; Neves, A.; Nuber, B.; Weiss, J. *Inorg. Chem.* **1989**, *28*, 432.
(7) (a) Neubold, P.; Wieghardt, K.; Nuber, B.; Weiss, J. *Angew. Chem., Int. Ed. Engl.* **1988**, *27*, 933. (b) Neubold, P.; Wieghardt, K.; Nuber, B.; Weiss, J. *Inorg. Chem.* **1989**, *28*, 459.
(8) Armstrong, W. H.; Lippard, S. J. *J. Am. Chem. Soc.* **1984**, *106*, 4632.
(9) Chaudhuri, P.; Winter, M.; Küppers, H.-J.; Wieghardt, K.; Nuber, B.; Weiss, J. *Inorg. Chem.* **1987**, *26*, 3302.
(10) Turowski, P. N.; Bino, A.; Lippard, S. J. *Angew. Chem., Int. Ed. Engl.* **1990**, *29*, 841.
(11) Wieghardt, K.; Chaudhuri, P.; Nuber, B.; Weiss, J. *Inorg. Chem.* **1982**, *21*, 3086.

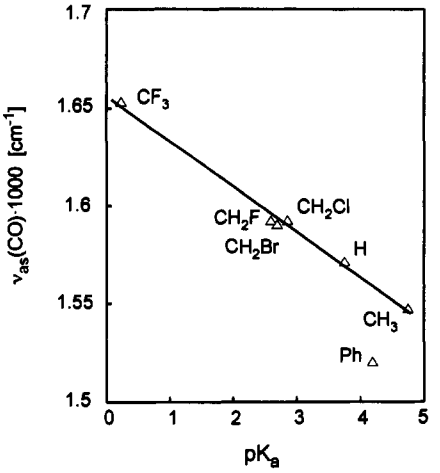

Figure 2. Correlation between the antisymmetric C–O stretching frequency of $[L_2V_2(\mu\text{-O})(\mu\text{-carboxylato})_2]^{2+}$ complexes and the dissociation constant of uncoordinated carboxylic acids (R–COOH).

bis[(1,4,7-trimethyl-1,4,7-triazacyclononane)vanadium(III)] dications. The hexafluorophosphate or iodide salts can be precipitated by addition of KPF_6 and NaI, respectively. In this work we have characterized the trifluoroacetato, fluoroacetato, chloroacetato, bromoacetato, and formato complexes for the first time whereas the acetato and benzoato species have been described previously and the crystal structure of $[L_2V_2(\mu\text{-O})(\mu\text{-}CH_3CO_2)_2]I_2\cdot 2H_2O$ has been reported.[2]

The electronic spectra of these compounds are very similar and characteristic for the (μ-oxo)bis(μ-carboxylato)divanadium(III) core. Three very intense absorption maxima in the visible region are observed at 660–710, 450–460, and in some cases 260–275 nm, all of which have molar absorption coefficients >2000 L mol^{-1} cm^{-1} (Figure 1). The magnetic properties of the acetato complex have been reported.[2c] A temperature-independent (10–300 K) magnetic moment of 4.82 μ_B per dinuclear unit (3.41 μ_B/V) is indicative of a strong intramolecular ferromagnetic coupling yielding an $S = 2$ ground state. It has been estimated that, within the isotropic Heisenberg–Dirac–van Vleck model for spin-exchange coupling using the Hamiltonian $\mathbf{H} = -2JS_1\cdot S_2$ ($S_1 = S_2 = 1$), the lower limit for J is +200 cm^{-1}.[2c] From eq 2, where n_{tot} represents

$$\mu_{eff} = [n_{tot}(n_{tot} + 2)]^{1/2} \qquad (2)$$

$$n_{tot} = n_a + n_b \qquad n_a = n_b = 2$$

the sum of unpaired electrons of metal ion a (n_a) and metal ion b (n_b) in a dinuclear complex with fully aligned spins of all unpaired electrons, a spin-only value of 4.90 μ_B per dinuclear unit (or 3.465 μ_B/V) is calculated, which is close to the observed magnetic moment. From susceptibility measurements on powdered samples of the fluoroacetato, bromoacetato, trifluoroacetato, and benzoato complexes in the temperature range 90–298 K temperature-independent magnetic moments of 4.6, 4.7, 4.85, and 4.9 μ_B per dinuclear complex were calculated, respectively. Thus we conclude that all (μ-oxo)bis(μ-carboxylato)divanadium(III) species have an $S = 2$ ground state.

The ν_{as}(C–O) stretching frequency of these complexes decreases with increasing pK_a value of the uncoordinated free carboxylic acid (Figure 2). Similar linear relationships have previously been observed for bis(μ-hydroxo)(μ-carboxylato)dicobalt(III)[12] complexes and their chromium(III)[13] analogues as well as for the (μ-oxo)bis(μ-carboxylato)diruthenium(III) complexes;[7] they are an indication of the electron-withdrawing capacity of the R group of the respective carboxylic acid. The same correlation may be constructed by using Taft's inductive parameter, σ_I, for the R groups.[14]

(12) Wieghardt, K. *J. Chem. Soc., Dalton Trans.* **1973**, 2548.
(13) Springborg, J.; Toftlund, H. *Acta Chem. Scand.* **1979**, *A33*, 31.

Table I. Formal Redox Potentials for $[L_2V_2(\mu\text{-O})(\mu\text{-carboxylato})_2]^{2+}$ Species in CH_3CN (0.1 M $[TBA]PF_6$ Supporting Electrolyte) at 20 °C

complex	$E^1_{1/2}$, V vs Fc^+/Fc	$E^2_{1/2}$, V vs Fc^+/Fc	ref
$CF_3CO_2^-$	+0.58	−1.43	this work
$FCH_2CO_2^-$	+0.16	−1.71	this work
$ClCH_2CO_2^-$	+0.18	−1.85	this work
$BrCH_2CO_2^-$	+0.21	−1.81	this work
$C_6H_5CO_2^-$	+0.21	−1.80	2c
$CH_3CO_2^-$	−0.02	−1.87	2c

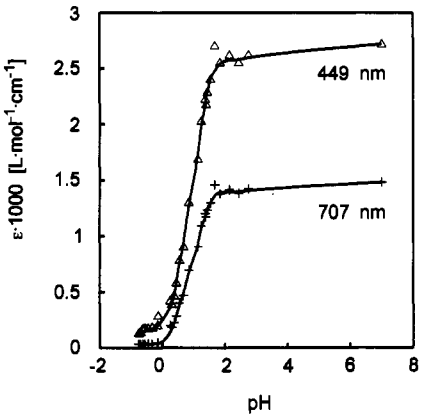

Figure 3. Absorption spectra at 449 and 707 nm of $[L_2V_2(\mu\text{-O})(\mu\text{-}CH_3CO_2)_2]I_2\cdot 2H_2O$ as a function of pH ($[H^+] = 2.0\text{–}10^{-7}$ M) in perchloric acid media at 20 °C.

Figure 10 in ref 2c shows the cyclic voltammogram of $[L_2V_2(\mu\text{-O})(\mu\text{-}CH_3CO_2)_2](PF_6)_2$; this is representative for the whole series of carboxylato-bridged complexes of this work. Measurements in CH_3CN (0.1 M $[TBA]PF_6$ supporting electrolyte, Au-disk working electrode) in the range −2.10 to +1.6 V vs Ag/AgCl exhibit two reversible one-electron-transfer waves, which have been shown to correspond to the formation of $V^{III}V^{IV}$ and $V^{III}V^{II}$ mixed-valence species (eq 3). Table I summarizes

$$V^{III}V^{IV} \underset{-e^-}{\overset{e^-}{\rightleftharpoons}} V^{III}{}_2 \underset{-e^-}{\overset{+e^-}{\rightleftharpoons}} V^{III}V^{II} \qquad (3)$$
$$E^1_{1/2} \qquad E^2_{1/2}$$

the numerical values for $E^1_{1/2}$ and $E^2_{1/2}$. From these values a trend between the $E^1_{1/2}$, $E^2_{1/2}$, and Taft's inductive parameter, σ_I, for the R group of the carboxylato bridges is observed. With increasing electron-withdrawing capacity of R (Ph < CH_3 < H < $BCH_2 \lesssim ClCH_2 < FCH_2 \ll CF_3$), it becomes more difficult to oxidize the $V^{III}{}_2$ species and $E^1_{1/2}$ becomes more positive. In contrast, with increasing electron-withdrawing capacity of R, it is easier to reduce the $V^{III}{}_2$ complexes and $E^2_{1/2}$ becomes less negative. For $[L_2Ru^{III}{}_2(\mu\text{-O})(\mu\text{-carboxylato})_2]^{2+}$ complexes it has been shown that a linear correlation between these redox potentials and the σ_I (or pK_a) values exists.[7]

When an acetonitrile solution of one of these (μ-oxo)bis(μ-carboxylato)divanadium(III) complexes is treated with concentrated $HClO_4$ or HBr, a dramatic color change from green to red occurs. This process is completely reversible; neutralization of the acid restores the green color. We have been able to isolate red microcrystalline solid materials from such solutions in the case of the acetato and benzoato species. Elemental analyses and spectroscopic properties are in accord with their formulations as $[L_2V^{III}{}_2(\mu\text{-OH})(\mu\text{-}CH_3CO_2)_2](ClO_4)_3\cdot H_2O$ and $[L_2V^{III}{}_2(\mu\text{-OH})(\mu\text{-}C_6H_5CO_2)_2]Br_3$. Both solids are very hygroscopic; they dissolve in H_2O with a green color and release of protons. We have not been able to grow single crystals suitable for an X-ray

(14) Values for acid dissociation constants, pK_a, were taken from: Kortüm, G.; Vogel, W.; Andrussow, K. *Dissociation Constants of Organic Acids in Aqueous Solutions*; Butterworths: London, 1961. For a compilation of Taft's inductive parameters, σ_I, see: *Correlation Analysis in Chemistry*; Plenum Press: New York and London, 1978; Chapter 10.

Table II. Comparison of Structural and Magnetic Properties of Homodinuclear (μ-Oxo)bis(μ-carboxylato)dimetal(III) and (μ-Hydroxo)bis(μ-carboxylato)dimetal(III) Complexes

no.	complex[a]		M··M, Å	M–O_b, Å	magnetism, J, cm^{-1}	ref
1	$[L_2Ti^{III}_2O(PhCO_2)_2]^{2+}$	d^1–d^1	3.198 (4)	1.80 (2)	diamagnetic[b]	1
2	$[L_2V^{III}_2O(CH_3CO_2)_2]^{2+}$	d^2–d^2	3.250 (2)	1.792 (4)	>+200	2
3	$[L_2Cr^{III}_2O(CH_3CO_2)_2]^{2+}$	d^3–d^3	3.219 (2)	1.850 (5)	−28	3
4	$[L_2Mo^{III}_2O(CH_3CO_2)_2]^{2+}$	d^3–d^3	2.885 (1)	1.945 (4)	diamagnetic[b]	6
5	$[L_2Mn^{III}_2O(CH_3CO_2)_2]^{2+}$	d^4–d^4 (hs)	3.096 (2)	1.810 (4)	+9	4
6	$[L_2Fe^{III}_2O(CH_3CO_2)_2]^{2+}$	d^5–d^5 (hs)	3.120 (4)	1.800 (3)	−119	5
7	$[L_2Ru^{III}_2O(CH_3CO_2)_2]^{2+}$	d^5–d^5 (ls)	3.258 (1)	1.884 (2)	diamagnetic[b]	7
8	$[L_2V^{III}_2(OH)(PhCO_2)_2]^{3+}$	d^2–d^2			−36	this work
9	$[L_2Cr^{III}_2(OH)(CH_3CO_2)_2]^{3+}$	d^3–d^3			−15.5	9
10	$[(H_2O)_6Cr^{III}_2(OH)(HCO_2)_2]^{3+}$	d^3–d^3	3.381 (1)	1.919 (4)	−11.2	10
11	$[L_2Mo^{III}_2(OH)(CH_3CO_2)_2]^{3+}$	d^3–d^3	3.555 (1)	2.102 (7)	−96	6a
12	$[(HB(pz)_3)_2Fe^{III}_2(OH)(CH_3CO_2)_2]^{+}$	d^5–d^5 (hs)	3.439 (1)	1.956 (4)	−17	8
12	$[L_2Ru^{III}_2(OH)(CH_3CO_2)_2]^{3+}$	d^5–d^5 (ls)	3.472 (2)	1.98 (2)	−218	7

[a] L = 1,4,7-trimethyl-1,4,7-triazacyclononane; $HB(pz)_3$ = hydrotris(1-pyrazolyl)borate(1−); Ph = phenyl. [b] S = 0 ground state; $|J| > 400$ cm^{-1}.

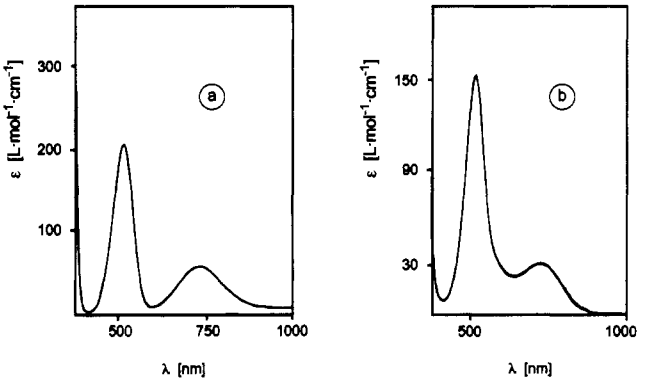

Figure 4. Electronic spectra of (a) $[L_2V_2(\mu\text{-OH})(\mu\text{-}CH_3CO_2)_2]^{3+}$ in 1.5 M $HClO_4$ and (b) $LVCl_3$ in CH_3CN at 20 °C.

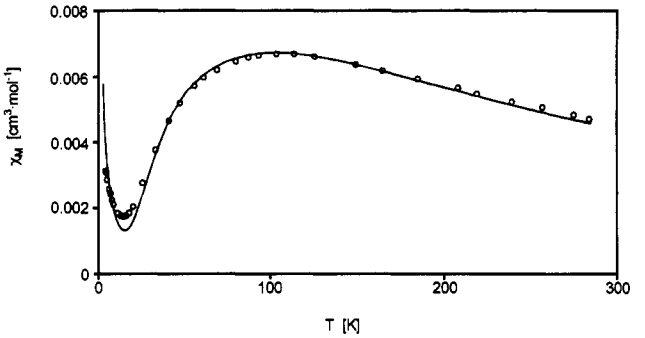

Figure 5. Molar susceptibility, χ_M, of $[L_2V_2(\mu\text{-OH})(\mu\text{-}O_2CC_6H_5)_2]Br_3$ as a function of the temperature, T. The solid line represents the best fit of data (O).

structure determination of either of these materials despite many attempts to do so. The equilibrium constant (acid dissociation constant K_a, eq 4) has been determined spectrophotometrically for the acetato complex.

$$[L_2V_2(\mu\text{-OH})(\mu\text{-}CH_3CO_2)_2]^{3+} \overset{K_a}{\rightleftharpoons} [L_2V_2(\mu\text{-O})(\mu\text{-}CH_3CO_2)_2]^{2+} + H^+ \quad (4)$$

Aqueous perchloric acid solutions of $[L_2V_2(\mu\text{-O})(\mu\text{-}CH_3CO_2)_2]^{2+}$ were measured spectrophotometrically ($[H^+]$ = 2.0–10^{-1}7 M). Figure 3 shows the decrease in absorbance of the two intense absorption maxima of the μ-oxo-bridged species in the visible region at 449 and 707 nm as a function of increasing $[H^+]$. From the sigmoidal form a pK_a value of 0.9 ± 0.1 at 20 °C has been calculated.

The electronic spectrum of the fully protonated form $[L_2V_2(\mu\text{-OH})(\mu\text{-}CH_3CO_2)_2]^{3+}$ in 1.5 M $HClO_4$ is shown in Figure 4a. In the visible region two moderately intense absorption maxima are observed at 510 (220) and 735 nm (ϵ = 72 L mol^{-1} cm^{-1}). These bands may be assigned to d–d transitions ($^3T_1(F)$–$^3T_2(F)$, $^3T_1(F)$–$^3T_1(P)$) of a pseudooctahedral V(III) ion. They are very similar to those observed for the genuine monomer $LVCl_3$, which is shown in Figure 4b. Thus protonation of the μ-oxo group destroys the characteristic electronic spectrum of the (μ-oxo)bis(μ-carboxylato)divanadium(III) core and more conventional d–d transitions of individual octahedral vanadium(III) moieties are observed.

Figure 5 shows a plot of the molar susceptibility, χ_M, versus the temperature T for $[L_2V_2(\mu\text{-OH})(\mu\text{-}C_6H_5CO_2)_2]Br_3$. χ_M increases with decreasing temperature and reaches a maximum at ≈100 K. Then χ_M decreases with decreasing temperature and below ≈20 K increases sharply again. This behavior is typical for an antiferromagnetically coupled dinuclear species with an S = 0 ground state which contains a paramagnetic impurity. The solid line in Figure 4 represents the best fit of the data to the isotropic Heisenberg–Dirac–Van Vleck model by using the Hamiltonian $\mathbf{H} = -2JS_1 \cdot S_2$ ($S_1 = S_2 = 1$), with $J = -36$ cm^{-1}, g = 1.87, and a 0.1% paramagnetic impurity (S = 1). The impurity is most likely the deprotonated form. Similar behavior is observed for $[L_2V_2(\mu\text{-OH})(\mu\text{-}CH_3CO_2)_2](ClO_4)_3 \cdot H_2O$, for which χ_M was measured in the temperature range 78–298 K. An excellent fit of the data to the above model was obtained with J = −35 (2) cm^{-1} and g = 1.90. Thus we conclude that the dinuclear μ-OH-bridged V(III) complexes are intramolecularly antiferromagnetically coupled (S = 0 ground state), in contrast to their μ-oxo-bridged counterparts, which have an S = 2 ground state.

Discussion

For the discussion of the remarkable change of the intramolecular spin-exchange coupling in (μ-oxo)bis(μ-carboxylato)divanadium(III) complexes upon protonation of the oxo bridge, we have assembled pertinent structural data and the magnetism of a series of μ-oxo- and μ-hydroxo-bridged analogues in Table II. Armstrong and Lippard[8,15] reported the first pair of such complexes, namely $[(HB(pz)_3)_2Fe^{III}_2(\mu\text{-O})(\mu\text{-}CH_3CO_2)_2]^0$ and $[(HB(pz)_3)_2Fe^{III}_2(\mu\text{-OH})(\mu\text{-}CH_3CO_2)_2]^+$ where $HB(pz)_3^-$ is the hydrotris(pyrazolyl)borate anion. In both species two high-spin ferric ions (d^5) are antiferromagnetically coupled. For the μ-oxo complex J is −121 cm^{-1} whereas in the latter the coupling is very much reduced (J = −17 cm^{-1}) but still antiferromagnetic. We have described similar behavior for the couples $[L_2M_2(\mu\text{-O})(\mu\text{-}CH_3CO_2)_2]^{3+}$ and $[L_2M_2(\mu\text{-OH})(\mu\text{-}CH_3CO_2)_2]$ where M = Mo^{III} (d^3) and Ru^{III} (d^5, low spin).[6,7] The μ-oxo-bridged complexes of Mo(III) and Ru(III) are diamagnetic whereas the corresponding μ-hydroxo species are strongly antiferromagnetically coupled. Recently, we have also been able to show that in $[L_2Cr^{III}_2(\mu\text{-O})(\mu\text{-}CH_3CO_2)_2]^{2+}$ the two Cr(III) ions (d^3) are antiferromagnetically coupled (J = −28 cm^{-1})[3] as they are in the μ-hydroxo-bridged analogue $[L_2Cr^{III}_2(\mu\text{-OH})(\mu\text{-}CH_3CO_2)_2]^{3+}$,[9] where the coupling is only very little reduced (J = −15.5). In none of these examples has a change in the nature of the coupling, i.e. antiferromagnetic to ferromagnetic or vice versa, been observed.

(15) Armstrong, W. H.; Spool, A.; Papaefthymiou, G. C.; Frankel, R. B.; Lippard, S. J. *J. Am. Chem. Soc.* **1984**, *106*, 3653.

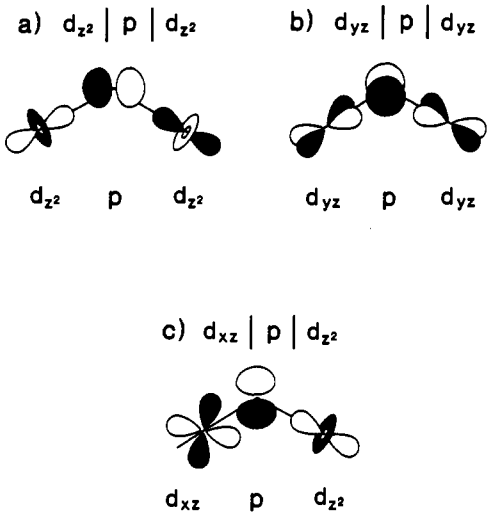

Figure 6. Sketch of the symmetry-allowed interactions between d atom orbitals and a p orbital of the oxo bridge in $[L_2M_2(\mu\text{-}O)(\mu\text{-carboxylato})_2]^{2+}$ complexes.

Inspection of the structural data in Table II reveals that the most dramatic structural change upon protonation is a significant lengthening of the metal–oxygen bond distance on going from μ-oxo to μ-hydroxo bridging. From these data the difference (M–O(hydroxo) – (M–O(oxo)) is 0.17 Å for the Fe(III), 0.16 Å for the Mo(III), and 0.10 Å for the Ru(III) couple. For the Cr(III) couple a difference of 0.07 Å may be estimated by using the M–O(hydroxo) distance determined for $[(H_2O)_6Cr_2(\mu\text{-}OH)(\mu\text{-}HCO_2)_2]^{3+}$.[10] A consequence of this bond lengthening is of course that the M···M distance also increases. In the light of these results, we feel that the same structural changes occur when the oxo bridges in the vanadium(III) complexes are protonated. The average V–O(alkoxo) distance distance in the μ-alkoxo-bridged complex $[H_2en][V(Hnhet)]_2{\cdot}2H_2O$[16] is 2.044 Å, which is longer by 0.25 Å than the V–O(oxo) distance in $[L_2V_2(\mu\text{-}O)(\mu\text{-}CH_3CO_2)_2]^{2+}$.

We qualitatively rationalize the magnetism of the complexes in Table II on the basis of the observed structural changes. We have recently shown[17] that for (μ-oxo)bis(μ-carboxylato)dimetal(III) complexes the following symmetry-allowed orbital interactions are to be considered (Figure 6): (a) the d_{z^2} atom orbitals of both metal ions may interact with a filled p orbital of the oxo bridge ($d_{z^2}|p|d_{z^2}$; σ-superexchange pathway); (b) two d_{yz} atom orbitals may interact with a p orbital of the oxygen atom ($d_{yz}|p|d_{yz}$; π-superexchange pathway); (c) there may be strong overlap between a d_{xz} orbital at metal 1, a p orbital of the O^{2-} ion, and a d_{z^2} orbital at metal 2 ($d_{xz}|p|d_{z^2}$). Note that the z axis coincides with the M–O(oxo) bond vector and the x and y axes are directed along N–M–O(acetate) bonds, assuming ideal octahedral symmetry for the N_3MO_3 polyhedron in $[L_2M_2(\mu\text{-}O)(\mu\text{-}CH_3CO_2)_2]^{2+}$ complexes. In the oxo-bridged complexes the M–O(oxo) bond is always the shortest and, consequently, the d_{z^2} orbital is strongly destabilized, followed by the $d_{x^2-y^2}$ orbital; these are followed by the d_{yz} and d_{xz} orbitals, which are degenerate, and, finally, the d_{xy} orbital. From extended Hückel calculations for the $[N_5Fe(\mu\text{-}O)(\mu\text{-}HCO_2)_2FeN_5]^{2+}$ core it was calculated[17b] that in pathway c there is good overlap on the oxo bridge, affording an effective magnetic superexchange pathway. This is followed by pathways b and a. We have termed the $d_{xz}|p|d_{xz}$ interaction the "crossed pathway" because it involves overlap between a t_{2g} orbital at metal 1 and an e_g orbital at metal 2 and vice versa. Electronically two important situations are to be considered for

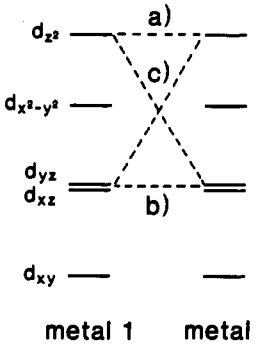

Figure 7. Schematic representation of the energetic order (arbitrary energy scale) of d orbitals and symmetry-allowed spin-exchange coupling pathways in $[L_2M_2(\mu\text{-}O)(\mu\text{-carboxylato})_2]^{2+}$ complexes.

Scheme I

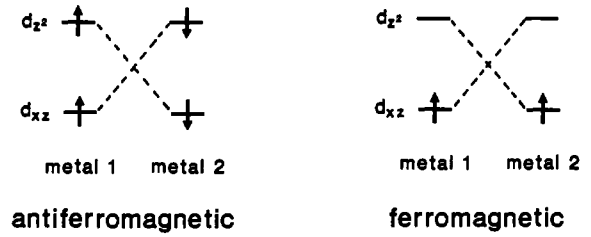

the crossed pathway (Scheme I): (i) if all four d atom orbitals—two at each metal ion—are half-filled, then an *antiferromagnetic* coupling mediated by the O^{2-} bridge is observed; (ii) if, on the other hand, only one d atom orbital at each metal is half-filled and the other is empty, the electronic coupling is *ferromagnetic* according to the Goodenough–Kanamori rules for magnetic superexchange.[18]

The sign of the intramolecular spin-exchange coupling constant J results then from the sum of antiferromagnetic and ferromagnetic contributions (eq 5). Figure 7 shows a schematic repre-

$$J = J_{AF} + J_F \tag{5}$$

sentation of the energetic order of the d orbitals within the (μ-oxo)bis(μ-carboxylato)dimetal(III) core and the exchange coupling pathways. For two high-spin ferric ions (d^5) it is evident that all three interactions provide antiferromagnetic contributions. Thus the Fe^{III}_2 species is the most strongly antiferromagnetically coupled system[5] within the series d^2–d^2, d^3–d^3, d^4–d^4 (hs), and d^5–d^5 (hs). Removal of two electrons from the d_{z^2} orbitals, i.e. going to the Mn^{III}_2 (d^4–d^4 hs) species, eliminates interaction a, and we are left with interactions b and c, the former of which provides an antiferromagnetic contribution and the latter of which a ferromagnetic contribution. Thus, according to eq 5, the net interaction may be antiferromagnetic, ferromagnetic, or apparently uncoupled when $J_{AF} = J_F$. Examples for all three cases have been reported.[4] Removal of two further electrons results in the Cr_2^{III} (d^3–d^3) case.[3] Both electrons are removed from the noninteracting $d_{x^2-y^2}$ orbitals, and in principle, the same situation is encountered as described for the Mn^{III}_2 dinuclear species. It must be kept in mind that the actual magnitudes of J_{AF} and J_F, although not explicitly known, are strongly dependent on the respective orbital overlap (magnitude of β coefficients in the Hückel theory) and these are dependent on the nature of the metal ion and—very importantly—on the actual M–O(oxo) bond length. Interaction c is expected to be especially sensitive to the latter point. The Cr–O(oxo) bond is longer (1.85 Å) than in the other complexes, and this may lead to a substantial weakening of ferromagnetic interaction c, yielding

(16) Shepherd, R. E.; Hatfield, W. E.; Ghosh, D.; Stout, C. D.; Kristine, F. J.; Ruble, J. R. *J. Am. Chem. Soc.* **1981**, *103*, 5511.

(17) (a) Bossek, U.; Weyhermüller, T.; Wieghardt, K.; Bonvoisin, J.; Girerd, J. J. *J. Chem. Soc., Chem. Commun.* **1989**, 633. (b) Hotzelmann, R.; Wieghardt, K.; Flörke, U.; Haupt, H.-J.; Weatherburn, D.; Bonvoisin, J.; Blondin, G.; Girerd, J. J. Submitted for publication.

(18) (a) Ginsberg, A. P. *Inorg. Chim. Acta Rev.* **1971**, *5*, 45. (b) Hatfield, W. E. In *Theory and Applications of Molecular Paramagnetism*; Boudreaux, E. A., Mulay, L. N., Eds.; Wiley: New York, 1976; p 349. (c) Anderson, P. W. *Phys. Rev.* **1959**, *115*, 2. (d) Anderson, P. W. In *Solid State Physics*; Seitz, F., Turnbull, D., Eds.; Academic Press: New York, 1963; p 99. (e) Goodenough, J. B. *Magnetism and the Chemical Bond*; Wiley: New York, 1963; p 165.

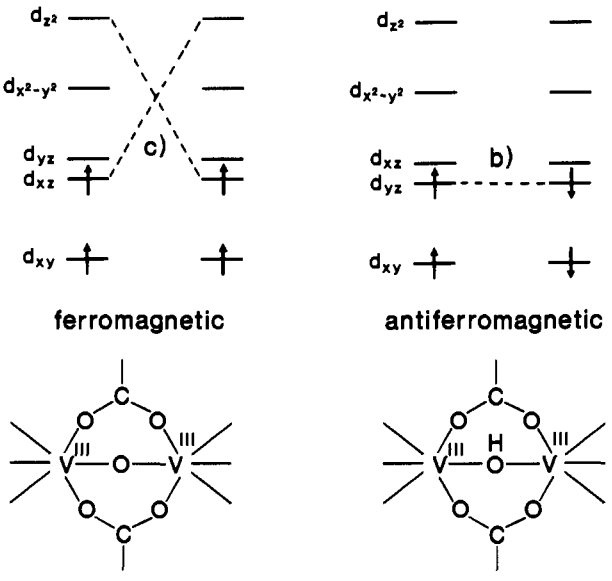

Figure 8. Schematic representation of spin-exchange pathways in $[L_2V_2(\mu\text{-O})(\mu\text{-carboxylato})_2]^{2+}$ and $[L_2V_2(\mu\text{-OH})(\mu\text{-carboxylato})_2]^{3+}$ complexes.

overall weak antiferromagnetic coupling.

We now turn to the interesting d^2–d^2 pair (V^{III}_2). Since the d_{xz} and d_{yz} atom orbitals are approximately degenerate, there exists a choice of two electronic configurations at each V(III) ion: $d_{xy}^1d_{xz}^1$ and $d_{xy}^1d_{yz}^1$. The $d_{yz}|p|d_{yz}$ interaction b would then yield strong antiferromagnetic coupling whereas the $d_z^2|p|d_{xz}$ interaction c would afford a very strong ferromagnetic interaction—as is experimentally observed. We therefore suggest that the degeneracy of the d_{yz} and d_{xz} orbitals is lifted probably due to lower symmetry of the V^{III}_2 dinuclear complexes or as a consequence of spin–orbit coupling. If the d_{xz} orbitals are energetically more favorable than the d_{xy} orbitals of the two vanadium(III) ions, the only available superexchange pathway would be c, which leads to ferromagnetic coupling (Figure 8). We have as yet no experimental evidence that this is the case, but it would explain qualitatively the observed magnetism in accord with the molecular orbital scheme discussed so far.

Weakening of the M–O(oxo) bond by protonation of the O^{2-} bridge decreases the orbital overlap of the d|p|d interactions a and b, but most dramatically that of interaction c (Figure 6) because the added proton removes electron density from the oxygen and weakens thereby its M=O π-donor capacity. As a consequence, interaction c is not effective any more. For $\{Fe^{III}(\mu\text{-OH})Fe^{III}\}$ complexes all three antiferromagnetic interactions are weaker and interaction c may altogether not be existent. In agreement with this prediction, the μ-OH-bridged species is only very weakly antiferromagnetically coupled.[8] No complexes containing a (μ-hydroxo)bis(μ-carboxylato)dimanganese(III) core have been reported to date. For Cr^{III}–OH–Cr^{III} complexes only pathway b is available, assuming pathway c to be nonexistent, and consequently, weak antiferromagnetic coupling is observed in complexes with a (μ-hydroxo)bis(μ-carboxylato)dichromium(III) core.[9,10] Since $[L_2V_2(\mu\text{-OH})(\mu\text{-OH}_3CO_2)_2]^{3+}$ displays antiferromagnetic coupling, we propose a reversal of the energetic order of the d_{yz} and d_{xz} orbitals, with d_{yz} being more favorable (Figure 8). The $d_{yz}|p|d_{yz}$ interaction b provides then a superexchange pathway for spin-exchange coupling, leading to antiparallel spin alignment.

In essence, we propose that, in (μ-hydroxo)bis(μ-carboxylato)dimetal(III) complexes containing two first-row transition-metal ions with a d^2, d^3, d^4, and d^5 electron configuration, the classical $d_{yz}|p|d_{yz}$ superexchange pathway is dominant. This is in agreement with the fact that only antiferromagnetic coupling has been observed for these complexes.[9] There is no example for ferromagnetic coupling known.

It is interesting to note the obvious discrepancy observed for the d^1–d^1 pair (Ti^{III}_2),[1] for which the above scheme predicts and uncoupled behavior (paramagnetism), but in fact $[L_2Ti^{III}_2(\mu\text{-O})(\mu\text{-C}_6H_5CO_2)_2]^{2+}$ is diamagnetic. We have ascribed this to a direct through-space interaction of the somewhat larger d_{xy} and d_{xy} orbitals, which might be termed an "incipient metal–metal bond":

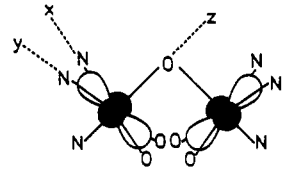

Metal–metal multiple bonding has been shown to exist in diamagnetic $[L_2Mo^{III}_2(\mu\text{-O})(\mu\text{-CH}_3CO_2)_2]^{2+}$, where the Mo–Mo distance is 2.885 (1) Å, which is shorter by ≈0.32 Å than in all other $[L_2M^{III}_2(\mu\text{-O})(\mu\text{-CH}_3CO_2)_2]^{2+}$ complexes (Table II). For diamagnetic $[L_2Ru^{III}_2(\mu\text{-O})(\mu\text{-CH}_3CO_2)_2]^{2+}$, the situation is borderline.[7] In both instances, protonation at the μ-oxo bridge leads to much larger M–M distances (Mo^{III}_2, 3.555 (1) Å; Ru^{III}_2, 3.472 (2) Å) with rupture of the metal–metal bond. Both hydroxo-bridged species display antiferromagnetic coupling in accord with the model outlined above (pathway b).

Acknowledgment. We thank Prof. W. Haase and co-workers (TH Darmstadt) for measuring the low-temperature susceptibility of $[L_2V_2(\mu\text{-OH})(\mu\text{-O}_2CC_6H_5)_2]Br_3$. We also thank the Fonds der Chemischen Industrie for financial support.

Registry No. $[L_2V_2(O)(O_2CCF_3)_2](PF_6)_2$, 136175-93-4; $[L_2V_2(O)(O_2CCH_2F)_2](PF_6)_2$, 136175-95-6; $[L_2V_2(O)(O_2CCH_2Cl)_2](PF_6)_2$, 136175-97-8; $[L_2V_2(O)(O_2CCH_2Br)_2](PF_6)_2$, 136175-99-0; $[L_2V_2(O)(O_2CH)_2]I_2$, 136176-00-6; $[L_2V_2(OH)(O_2CC_6H_5)_2]Br_3$, 136176-01-7; $[L_2V_2(OH)(O_2CCH_3)_2](ClO_4)_3$, 136176-03-9; $LVCl_3$, 112087-96-4; $[L_2V_2(O)(O_2CC_6H_5)_2]I_2$, 136176-04-0; $[L_2V_2(O)(O_2CCH_3)_2](ClO_4)_2$, 136176-05-1; $[L_2V_2(O)(O_2CCF_3)_2](PF_6)_2\cdot 2H_2O$, 136176-06-2; $[L_2V_2(O)(O_2CCH_2F)_2](PF_6)_2\cdot 2H_2O$, 136176-07-3; $[L_2V_2(O)(O_2CH)_2]I_2\cdot 2H_2O$, 136176-08-4; O^{2-}, 16833-27-5; $[L_2V_2(O)(O_2CCF_3)_2]^{3+}$, 136176-09-5; $[L_2V_2(O)(O_2CCF_3)_2]^{+}$, 136176-10-8; $[L_2V_2(O)(O_2CCH_2F)_2]^{3+}$, 136176-11-9; $[L_2V_2(O)(O_2CCH_2F)_2]^{+}$, 136176-12-0; $[L_2V_2(O)(O_2CCH_2Cl)_2]^{3+}$, 136176-13-1; $[L_2V_2(O)(O_2CCH_2Cl)_2]^{+}$, 136176-14-2; $[L_2V_2(O)(O_2CCH_2Br)_2]^{3+}$, 136176-15-3; $[L_2V_2(O)(O_2CCH_2Br)_2]^{+}$, 136176-16-4.